ETH zürich

ETH Library

Cell type–specific expression of SEPT3-homology subgroup members controls the subunit number of heteromeric septin complexes

Journal Article

Author(s):
Sellin, Mikael E.; Stenmark, Sonja; Gullberg, Martin

Publication date:
2014-05-15

Permanent link:
https://doi.org/10.3929/ethz-b-000088155

Rights / license:
Creative Commons Attribution-NonCommercial-ShareAlike 3.0 Unported

Originally published in:
Molecular Biology of the Cell 25(10), https://doi.org/10.1091/mbc.E13-09-0553

This page was generated automatically upon download from the ETH Zurich Research Collection.
For more information, please consult the Terms of use.

Cell type–specific expression of SEPT3-homology subgroup members controls the subunit number of heteromeric septin complexes

Mikael E. Sellin[a,b], Sonja Stenmark[a], and Martin Gullberg[a]
[a]Department of Molecular Biology, Umeå University, SE-901 87 Umeå, Sweden; [b]Institute of Microbiology, D-BIOL, ETH Zürich, 8093 Zürich, Switzerland

ABSTRACT **Septins are filament-forming proteins important for organizing the cortex of animal and fungal cells. In mammals, 13 septin paralogues were recently shown to assemble into core heterohexamer and heterooctamer complexes, which serve as building blocks for apolar filamentous structures that differ among cell types. To determine how tissue-specific septin paralogue expression may shape core heteromer repertoires and thereby modulate properties of septin filaments, we devised protocols to analyze native septin heteromers with distinct numbers of subunits. Our evidence based on genetically manipulated human cells supports and extends recent concepts of homology subgroup–restricted assembly into distinct categories of apolar heterohexamers and heterooctamers. We also identify a category of tetramers that have a subunit composition equivalent to an octameric building block. These atypical tetramers are prevalent in lymphocytes and neural tissues, in which octamers are abundant but hexamers are rare. Our results can be explained by tissue-specific expression of SEPT3 subgroup members: SEPT3, SEPT9, and SEPT12. These serve as cognate subunits in either heterooctamers or atypical tetramers but exhibit different preferences in various tissues. The identified tissue-specific repertoires of septin heteromers provide insights into how higher-order septin structures with differential properties and stabilities may form in diverse animal cell types.**

Monitoring Editor
Doug Kellogg
University of California, Santa Cruz

Received: Sep 26, 2013
Revised: Mar 3, 2014
Accepted: Mar 11, 2014

INTRODUCTION

Septins are a family of GTP-binding and membrane-interacting cytoskeletal proteins proposed to organize the cortex of fungal and animal cells. Septins polymerize at the contractile ring, where they may serve as membrane-diffusion barriers and/or molecular scaffolds during cytokinesis (reviewed in Beise and Trimble, 2011). By analogy with septin localization at the neck of the emerging bud of budding yeast (reviewed in McMurray and Thorner, 2009), septin filaments have been detected at the base of cellular appendices such as dendritic spines, flagellae, and cilia and appear to have essential functions at these locations (Ihara *et al.*, 2005; Kissel *et al.*, 2005; Tada *et al.*, 2007; Xie *et al.*, 2007; Hu *et al.*, 2010). This suggests that septins have a conserved role in insulating the base of cell appendages. In addition, septins are also associated with actin bundles and microtubules in nondividing mammalian cells (reviewed in Mostowy and Cossart, 2012).

Hallmarks of septin proteins include a conserved "G domain" flanked by variable N- and C-termini. Paralogous septins assemble into rod-shaped heteromeric complexes, which contain four, six, or eight subunits, depending on the organism (Field *et al.*, 1996; John *et al.*, 2007; Sirajuddin *et al.*, 2007; Bertin *et al.*, 2008; Sellin *et al.*, 2011b). These complexes represent core hetero-oligomeric building blocks that assemble into filaments via longitudinal and lateral interactions (reviewed in Weirich *et al.*, 2008). Crystal structures of human septins expressed in *Escherichia coli* led to identification of two interaction interfaces—denoted the G and N-C interfaces—located on opposite sides of the GTP-binding G domain (Sirajuddin *et al.*, 2007). Each septin associates with its neighbors through either a G

This article was published online ahead of print in MBoC in Press (http://www.molbiolcell.org/cgi/doi/10.1091/mbc.E13-09-0553) on March 19, 2014.

Address correspondence to: Martin Gullberg (martin.gullberg@molbiol.umu.se).

Abbreviations used: EBV, Epstein-Barr virus; Flag-SEPT3, SEPT3 fused to an eight-amino-acid Flag tag; Flag-SEPT12, SEPT12 fused to an eight-amino-acid Flag tag; G-domain, GTP-binding domain; GTP, guanosine 5′-triphosphate; SEPT7-AcGFP, SEPT7 with a C-terminal Aequorea coerulescens green fluorescent protein reporter; shRNA, short hairpin RNA.

© 2014 Sellin *et al.* This article is distributed by The American Society for Cell Biology under license from the author(s). Two months after publication it is available to the public under an Attribution–Noncommercial–Share Alike 3.0 Unported Creative Commons License (http://creativecommons.org/licenses/by-nc-sa/3.0).
"ASCB®," "The American Society for Cell Biology®," and "Molecular Biology of the Cell®" are registered trademarks of The American Society of Cell Biology.

or an N-C interface. In this way, septins assemble into hetero-oligomeric protomer units, which in turn may form extended filaments by cognate interactions between terminal septin subunits.

Based on mutations and genetic rearrangements, septin dysfunction has been linked to a number of disease states, including tumors and hereditary neuralgic amyotrophy (reviewed in Mostowy and Cossart, 2012). However, identification of molecular mechanisms is hampered by the multitude of paralogous septin gene products—7 in most yeast species and 9–17 in vertebrates—which in some cases may replace each other in heteromeric complexes (Kinoshita, 2003; Cao *et al.*, 2007; Sellin *et al.*, 2011b). Mammals have 13 genes encoding both ubiquitous and tissue-specific septin paralogues: SEPT1 to SEPT12 and SEPT14, which are classified into four homology-based subgroups named after their founding members, SEPT2, SEPT3, SEPT6, and SEPT7 (Figure 1A; Kinoshita, 2003). Only two or three of these subgroups are represented among invertebrates, and phylogenetic analysis does not indicate an orthologous relationship between septin paralogues of animals and fungi (Cao *et al.*, 2007; Pan *et al.*, 2007).

Homology-based classification of animal septins predicts septin-pairing preferences, which was originally suggested by recombinant coexpression of human septin paralogues in various combinations. These studies suggested homology subgroup–restricted pairing preferences between the SEPT2 and SEPT6 subgroup members, and that SEPT7—the sole member of its subgroup—is essential for assembly of heterohexamers (Kinoshita *et al.*, 2002; Kinoshita, 2003; Mendoza *et al.*, 2002; Sheffield *et al.*, 2003). Subsequent analysis of the native assembly states of individual septins in a human cell model system substantiated these findings and further indicated that septin hetero-oligomerization is subgroup directed to the final configurations of both hexameric and octameric core heteromers (Sellin *et al.*, 2011b). Evidence supporting this model includes subgroup-restricted competition for available hetero-oligomerization partners during assembly of heterohexamers and heterooctamers, which both contain SEPT2 and SEPT6 subgroup members and SEPT7, whereas the heterooctamers additionally contain SEPT9. Consistently, hexamer-to-octamer ratio in the model myeloid leukemia cell line used is controlled by the substoichiometric amount of SEPT9, which in turn modulates higher-order arrangements of the septin system (Sellin *et al.*, 2012).

When coexpressed in *E. coli*, the SEPT2, SEPT6, and SEPT7 proteins form a linear SEPT7-SEPT6-SEPT2-SEPT2-SEPT6-SEPT7 heterohexamer, which is arranged as an apolar head-to-head trimer (Sirajuddin *et al.*, 2007). A subsequent study (Sirajuddin *et al.*, 2009) addressed the significance of alternating intrinsic GTPase activity among septin subunits, which was found to be consistent with the idea that all the members of the SEPT2 and SEPT6 subgroups may replace their cognate founding members in heterohexamers capped by SEPT7 (the sole member of its subgroup). Recent evidence, which includes mutational analysis of interaction surfaces (Kim *et al.*, 2011) and the finding that SEPT9—in contrast to other septins—exists as monomers in cells lacking SEPT7 (Sellin *et al.*, 2011b), supports the idea that SEPT9 caps the ends of octamers via a G interface with SEPT7.

The findings just outlined suggest that the multiple members of the SEPT2 and SEPT6 subgroups are arranged according to their respective subgroup in the center of both hexamers and octamers. However, whether the members of the SEPT3 subgroup (SEPT3, SEPT9, and SEPT12) serve as replaceable subunits at octamer ends has not previously been investigated. Orthologues of these SEPT3 subgroup members exist only in vertebrates, with a subgroup-specific feature being the absence of a C-terminal coiled-coil motif (Cao *et al.*, 2007). Expression of SEPT3 and SEPT12 appears to be restricted to neural cells and sperms, respectively (Xue *et al.*, 2004; Steels *et al.*, 2007). SEPT9 is distinguished by a unique N-terminal extension that, due to alternative mRNA splicing, is variable among six confirmed isoform variants (Figure 1B). Whereas SEPT9 is detected in most cell types, expression levels and isoform compositions do vary, which has functional consequences (Estey *et al.*, 2010; Sellin *et al.*, 2012; Bai *et al.*, 2013).

As noted, current evidence suggests that the three SEPT3 subgroup members in vertebrates has tissue-specific functions. However, meaningful interpretation of their roles requires a clear understanding of their interdependence with other septins expressed within the cell. In this study we explore how differentially expressed septin paralogues may shape tissue-specific repertoires of core heteromers—the building blocks of septin filaments. The results corroborate previous evidence for homology subgroup–directed septin assembly into distinct subsets of stable heteromeric complexes. We also identify a SEPT3 subgroup–specific role in directing assembly of a category of tissue-specific tetramers. SEPT3 subgroup members are found to have very different propensities to generate tetramers and octamers in a human cell model system. Analysis of live cells reveals that the proportions of tetramers, hexamers, and octamers are of significance for the size of circular submembranous septin structures, which we propose may be a result of an increased stability of filaments composed of octamers as compared with hexamers and tetramers.

RESULTS

Blue native PAGE resolves septin heteromers according to subunit number and SEPT9 isoform composition

As outlined in the *Introduction*, mammals have 13 genes encoding both ubiquitous and tissue-specific septin paralogues, which are classified into four homology-based subgroups (Figure 1A). SEPT9 is the sole SEPT3 subgroup member detected in the human myeloid K562 cell line. Alternative mRNA splicing generates SEPT9 protein isoforms with a common G domain but variable N-terminal extensions. K562 cells express three SEPT9 isoforms in the proportions indicated in Figure 1B (Sellin *et al.*, 2012). As evidenced by previous hydrodynamic and single-particle data, K562 contains a mixture of heterohexamers and heterooctamers (ratio ~1:1), with octamers distinguished from hexamers by the additional presence of SEPT9 subunits (Sellin *et al.*, 2011b). The likely general subunit arrangement in these heteromeric complexes is depicted in Figure 1A.

We previously optimized conditions required for complete disassembly of higher-order septin structures into pools of soluble and stable core heteromers (Sellin *et al.*, 2011a,b). Figure 1C shows core heteromer pools in K562 cell extract analyzed by blue native PAGE, which resolves native protein complexes according to molecular mass and shape (Wittig *et al.*, 2006). Immunodetection of SEPT7, which is indicative of all (or most) heterohexamers and heterooctamers, revealed four complexes in control cells (Vec-Co) but only a single complex in cells persistently depleted of SEPT9 by RNA interference (shRNA^{SEPT9}). It can be deduced from previous results (Sellin *et al.*, 2011b) that this complex, labeled 6-mer, is composed of heterohexamers of SEPT2 and SEPT6 subgroup members and SEPT7.

To generate cell lines expressing a single specified SEPT9 isoform, we cotransfected K562 cells with shRNA^{SEPT9} and constructs expressing SEPT9 isoform derivatives that carry silent DNA mutations that render them immune to RNA interference. We used replicating vectors that confer hygromycin resistance, which facilitate rapid selection of homogeneous cell populations. Figure 1C shows the heteromer composition of cells in which all the endogenous

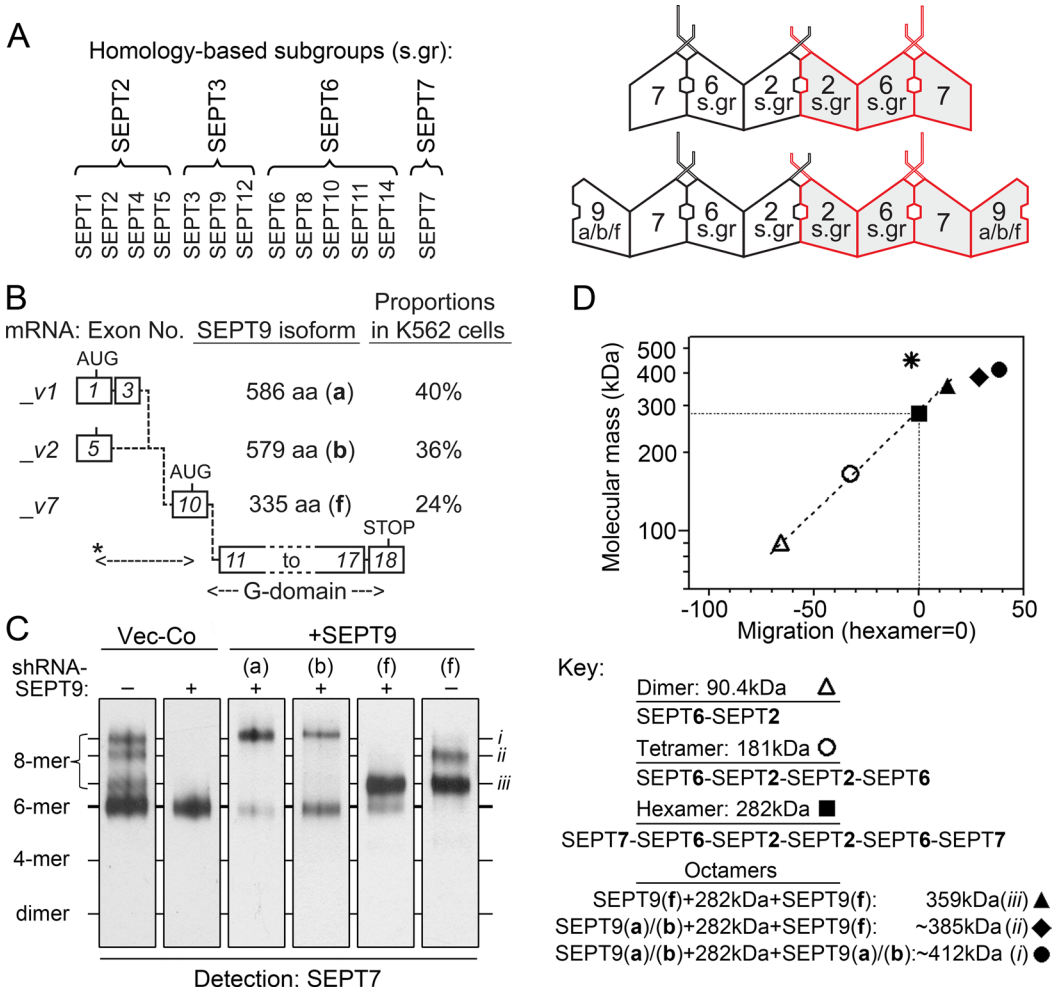

FIGURE 1: Blue native PAGE separation of human septin complexes according to subunit number and SEPT9 isoform. (A) Homology-based septin subgroups are depicted, which are named by founding members (adapted from Kinoshita, 2003). Note that former *SEPT13* is a pseudogene, *SEPT7P2*, HGNC:32339. Right, repertoire of hexameric and octameric core heteromers in K562 cells (modified from Sellin *et al.*, 2011b). The arrangement of SEPT2-subgroup (2-s.gr) and SEPT6-subgroup (6-s.gr) members, as well as of SEPT7, is according to the structure of a head-to-head SEPT2/6/7 trimer (PDB ID 2qag). The head-to-head arrangement around the central SEPT2s.gr-SEPT2s.gr N-C interface of octamers and hexamers is indicated (black to red). (B) SEPT9 transcript variants and protein isoforms expressed by the human myeloid K562 cell line. Splicing of the cognate coding exons (not drawn to scale) into the mRNA coding sequences (CDS) of *SEPT9* transcript variants (termed *_v1*, *_-v2*, and *_v7*). Exons corresponding to coding mRNA are depicted as boxes and numbered according to their order in the genome (exons *10–18* are common to all confirmed coding mRNAs). The length (aa, amino acids) of the cognate protein isoforms (a, b, and f) and their proportions in K562, as determined by quantitative Western blot, are indicated. Translation of isoform f starts at an in-frame AUG codon of exon *10*. The locations of the isoform-specific N-terminal extension (*) and G domain are indicated. (C) K562 cells were transfected with empty vector (Vec-Co), transfected with the replicating RNA interference vector shRNA^{SEPT9}, or cotransfected with shRNA^{SEPT9} and the indicated pMEP-SEPT9 isoform derivative, which all contain a silent mutation within the shRNA^{SEPT9}-targeted sequence. The analysis also included transfection of pMEP-SEPT9(f) alone. Cells were counterselected with hygromycin for ~1 wk, and expression levels were controlled as outlined in *Materials and Methods*. Septin heteromers of transfected cell lines were resolved by blue native PAGE, followed by immunodetection of SEPT7-containing heteromers. The proposed compositions of native octamers (8-mer, denoted *i, ii, and iii*) and hexamers (6-mer) are depicted in C. The indicated positions of tetramers (4-mer) and dimers are based on the migration of recombinant septin complexes shown in Supplemental Figure S1. (D) Correlation between molecular masses and the mobility of native (closed symbols, 8-mer and 6-mer; see B) and recombinant (open symbols, 4-mer and dimer; see Supplemental Figure S1) septin complexes as analyzed by blue native PAGE. Migration of the hexamer is set as 0; symbols indicate septin complexes as defined in the key. The migration of ferritin is also depicted (*450 kDa). The deduced molecular masses of the native octamers indicated were calculated with the assumption that all octamers are composed of the SEPT2-, SEPT6-, and SEPT7-containing hexamer capped with a SEPT9 protein at each end. Note that K562 cells express significant amounts of two and three members of the SEPT2 and SEPT6 subgroups, respectively, which may serve as alternative components of the hexamer; however, their molecular masses are similar to those of the founding member of each subgroup. Calculations were based on the following molecular masses: SEPT9(a), 65,401 Da; SEPT9(b), 64,681 Da; SEPT9(e), 47,501 Da; SEPT9(f), 38,518 Da; SEPT2, 41,487 Da; SEPT6 (isoform A), 48,872 Da; SEPT7(isoform 1), 50,679 kDa. The data are representative for cell lines derived from three independent transfections, which were analyzed by blue native PAGE on five occasions.

SEPT9 isoforms were replaced by a specified isoform. These data reveal that the endogenous complexes denoted *i–iii* correspond to octamers containing different SEPT9 isoforms. Thus expression of SEPT9(a), as well as of the similar-sized SEPT9(b) isoform, generates complex *i*, whereas SEPT9(f) generates complex *iii*. We also included ectopic expression of SEPT9(f) in cells retaining all the endogenous SEPT9 isoforms (i.e., not cotransfected with shRNA^{SEPT9}) in our analysis. Under these conditions, ectopic SEPT9(f) expression resulted in essentially complete depletion of the hexamer pool (6-mer) and alteration of the relative proportions of complexes *i–iii* to predominantly complexes *ii* and *iii* (Figure 1C, far right).

To correlate migration in blue native PAGE with the number of septin subunits, we also included recombinant dimers and tetramers of SEPT2 and SEPT6 in the analysis (Supplemental Figure S1). The migration of recombinant and native septin complexes is plotted against the molecular mass in Figure 1D. The results depict a log-linear relationship between the mobility and deduced mass of dimers, tetramers, hexamers, and SEPT9(f)-containing octamers (complex *iii*). This was as anticipated, since these complexes, which are depicted in Figure 1D, are composed of similar-sized septin paralogues. Figure 1D also illustrates that the ~282-kDa heterohexamer (■) migrates similarly to the globular ~450-kDa ferritin complex (*), which appears likely to reflect an elongated shape of septin heteromers. It is noteworthy that, relative to other septin complexes, the migration of SEPT9(a)- and SEPT9(b)-containing octamers (complex ***i***) was slower than predicted by their mass, which resulted in unexpectedly well-resolved heterooctamer subpopulations. As shown in Supplemental Table S1 and Supplemental Figure S2, this can be attributed to features of the isoform-specific N-terminal extension, which confer a disproportionately large increase in hydrodynamic volume on SEPT9.

Consistent with previous data, the analyses of K562 cells expressing a single defined SEPT9 isoform indicated that hetero-hexamers and heterooctamers are predominant, whereas heteroheptamers are rare or nonexistent. It is also notable that single transfection of the SEPT9(f) isoform results in an increase in both complex *ii* and complex *iii* (Figure 1C, far right). These data support the assignment of complex *ii* as octamers containing SEPT9(f) at one end and SEPT9(a) or SEPT9(b) at the other (Figure 1D, key).

Evidence that heterohexamers and heterooctamers comprise separate pools of mammalian septin heteromers

To study the structural integrity of core heteromers, we monitored the subunit number of heteromers after induced expression of ectopic SEPT9. The experimental protocol involved switching from suppression to induction of the hMTIIa promoter, which provides a transient burst of expression (Melander Gradin *et al.*, 1997; Sellin *et al.*, 2008). The SEPT9(f) isoform was chosen for this analysis since this is a minor isoform in K562 cells (~24% of total SEPT9; Figure 1B), and octamers containing SEPT9(f) subunits at both ends correspond to the low-abundance complex *iii* in control cells (Figure 1C). Analysis of cell extracts by SDS–PAGE and Western blotting demonstrated a transient burst of SEPT9(f) expression, which at early time points corresponds to a ~60-fold increase in the total SEPT9 content of cells (Figure 2A).

SEPT9 and other septins depend on appropriate hetero-oligomerization partners for optimal stability (Figure 3F; Kinoshita *et al.*, 2002; Sellin *et al.*, 2011b, 2012). Consequently, ectopic SEPT9 can be predicted to compete with endogenous SEPT9 for a limited number of appropriate of hetero-oligomerization partners, which has been shown to cause reduced cellular content of each one of the endogenous isoforms (Sellin *et al.*, 2012). Consistent with these

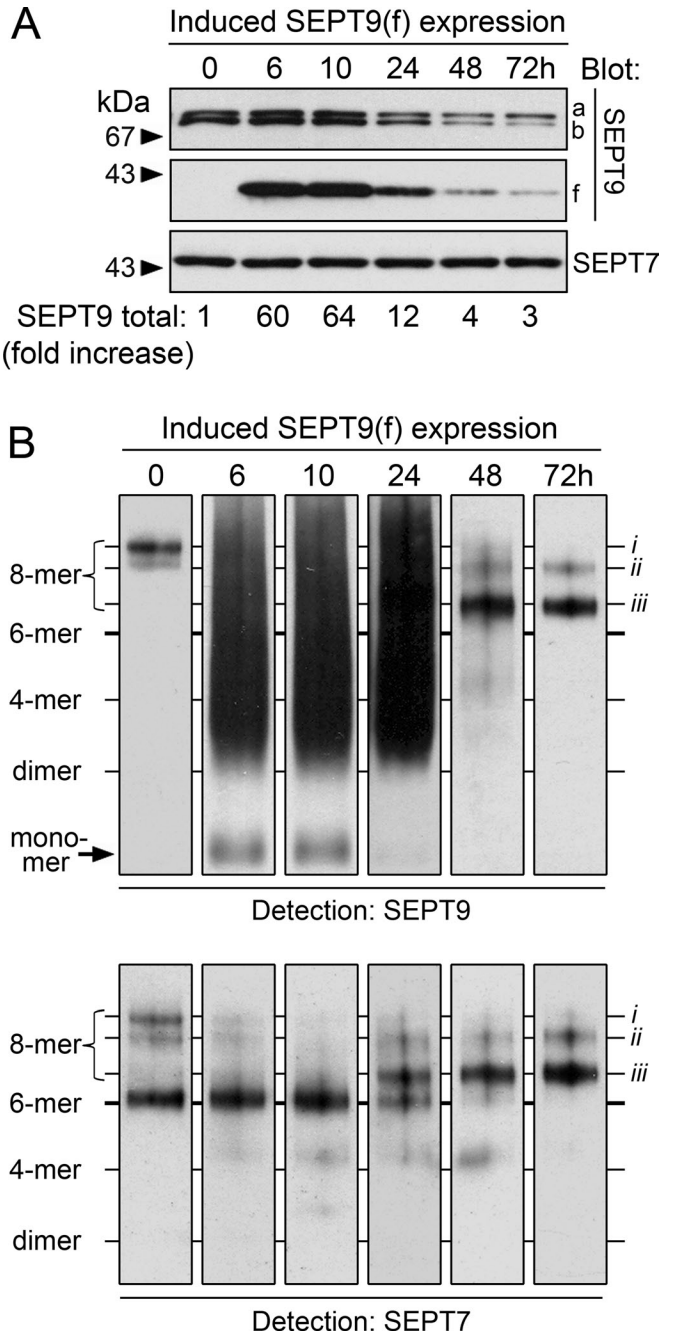

FIGURE 2: The assembly state of septins in cells induced to express a transient burst of SEPT9. K562 cells (cell cycle time, ~20 h) were transfected with pMEP-SEPT9(f) and counterselected with hygromycin for ~1 wk under conditions that suppress the hMTIIa promoter, and then high-level transient expression was attained as outlined in *Materials and Methods*. (A) Cells were harvested at the indicated time after induction of expression, and the content of SEPT9 and SEPT7 was analyzed by SDS–PAGE and Western blotting. Right, positions of SEPT9 isoforms. The relative increase in total SEPT9 content was determined by Western blotting of serially diluted extracts. The sum of the endogenous isoforms in Vector-Co cells was set as 1. (B) Same as A, but with the assembly state of septins monitored by blue native PAGE combined with detection of SEPT9 (top) and SEPT7 (bottom). Septin complexes are annotated according to Figure 1. The data are representative for cell lines derived from two independent transfections, which were analyzed by blue native PAGE on four occasions.

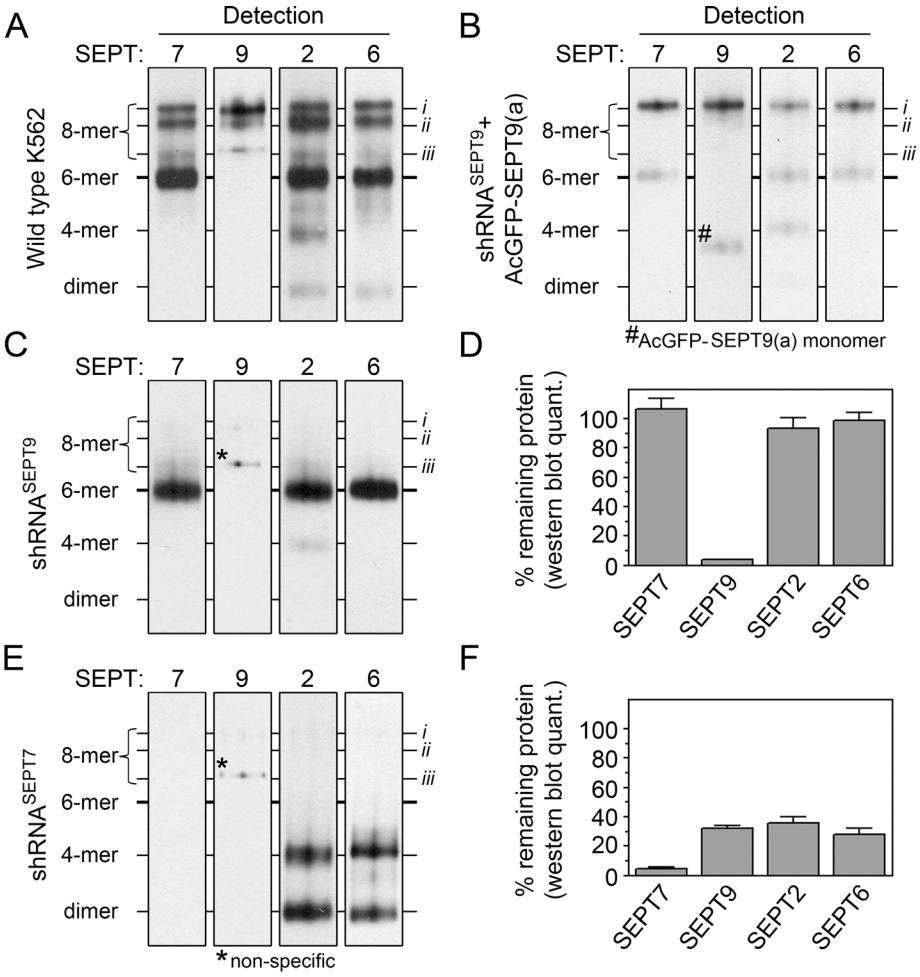

G

Wild type K562, 8-mer: **9**(a/b/f)-**7**-**6**s.gr-**2**s.gr-**2**s.gr-**6**s.gr-**7**-**9**(a/b/f)
6-mer: **7**-**6**s.gr-**2**s.gr-**2**s.gr-**6**s.gr-**7**

SEPT9-depleted, 6-mer: **7**-**6**s.gr-**2**s.gr-**2**s.gr-**6**s.gr-**7**

SEPT7-depleted, 4-mer: **6**s.gr-**2**s.gr-**2**s.gr-**6**s.gr
dimer: **6**s.gr-**2**s.gr

FIGURE 3: The subunit composition of heteromers with a specified number of subunits in control and genetically manipulated myeloid K562 cell lines. (A) Septin heteromers of normal K562 cells were resolved by blue native PAGE, followed by immunodetection of the septin homology subgroup representative indicated. Septin complexes are annotated according to Figure 1. (B) Cells with endogenous SEPT9 isoforms replaced by AcGFP-SEPT9(a) were analyzed as in A. Gene product replacement was attained by cotransfections with shRNA^{SEPT9} and pMEP-AcGFP-SEPT9(a) using the same general strategy and conditions as in Figure 1C. Note that the migration of AcGFP-SEPT9(a) monomers (indicated by #) is retarded by an extended N-terminus (Supplemental Figure S2B) and AcGFP-fusion partner. (C) SEPT9-depleted cells were analyzed as in A. Cell lines expressing shRNA^{SEPT9} were generated as in Figure 1C. Detection of SEPT9 revealed a nonspecific band (indicated by asterisk) after prolonged exposure. This band migrated close to complex *iii* but was not detected by any other septin antibody. (D) SDS–PAGE and Western blotting of serially diluted cell extract was used for quantification of the indicated septin in SEPT9-depleted cells (100% = the content of control cells). The estimated SEPT9 content represents the sum of all three endogenous isoforms. (E) SEPT7-depleted cells were analyzed as in A. Cell lines expressing shRNA^{SEPT9} were generated by the same general strategy as in C. Prolonged exposure revealed the same cross-reactive band as in C (indicated by asterisk). (F) SDS–PAGE and Western blotting were used for quantification of the indicated septin in SEPT7-depleted cells as in D. (G) Septin heteromers in wild-type and specifically depleted K562 cells. The arrangement of the indicated septin paralogue (homology subgroup, s.gr) is depicted as in Figure 1A. The head-to-head arrangement around the central SEPT2s.gr-SEPT2s.gr N-C interface of octamers and hexamers is indicated (black to red). SEPT9 isoforms are indicated within brackets. The data in A–F are representative for cell lines derived from two independent transfections, which were analyzed by blue native PAGE on four occasions.

previous findings, Western blots in Figure 2A show that induced SEPT9(f) expression caused a decrease in endogenous SEPT9(a) and SEPT9(b), whereas SEPT7 remained constant. K562 divides every ~20 h, but the procedure associated with induced expression causes an initial prolongation of the doubling time, which may account for the apparent delay at early time points in the decrease of endogenous SEPT9(a) and SEPT9(b).

Figure 2B shows blue native PAGE analysis of the assembly state of ectopic SEPT9(f) over a 72-h time course. Detection of SEPT9 (top) revealed a fraction of SEPT9(f) monomers at peak expression (6-10 h), but at these time points SEPT9 mainly existed as oligomers of various sizes that did not contain SEPT7 (bottom) or SEPT2 and SEPT6 (unpublished observations). Thus excessive overexpression caused aberrant homotypic SEPT9 interactions, but the resulting oligomers were unstable over time and undetectable after 48 h. The apparent decrease in octamers within the first 10 h, as detected by anti-SEPT7, suggested that septin interactions at excessive (nonphysiological) SEPT9 levels interfere with blue native PAGE analysis of heterooctamers. Most important, however, the heterohexamer pool as revealed by SEPT7 was initially unaffected by induced SEPT9 expression. These data demonstrate that preexisting hexamers remained unaltered even in the presence of excessive amounts of available SEPT9 subunits.

K562 divides every ~20 h, and each cell division means a twofold dilution of proteins present before induced SEPT9(f) expression. Figure 2B shows a gradual change in the hexamer-to-octamer ratio over a 48-h time span, which can be explained by dilution of preexisting heterohexamers by de novo–synthesized heterooctamers. As predicted by the assignment of complex *ii* as octamers containing SEPT9(f) at one end and any of the two large isoforms at the other (Figure 1D), Figure 2B reveals an increase in both complex *ii* and complex *iii*, accompanied by a decrease in complex *i*.

Given that an excess of newly synthesized SEPT9(f) has no immediate effect on the amounts of hexamers, it seems excluded that preexisting hexamers serve as assembly intermediates for octamers. This notion is

supported by an alternative experimental approach, which relied on induced expression of a fluorescent SEPT9 reporter (Supplemental Figure S3). Furthermore, we previously reported that hetero-hexamers do not readily exchange any of their subunits (Sellin *et al.*, 2011a). Hence, although these experiments do not exclude that subunit exchange may occur under certain conditions, our combined evidence supports the general idea that heterohexamers and heterooctamers comprise separate pools of mammalian septin heteromers.

Evidence for uniform subgroup-restricted septin pairing in heterohexamers and heterooctamers

As demonstrated in the preceding sections, blue native PAGE combined with immunodetection provides a means of determining the subunit composition of stable septin complexes with a specified number of subunits. We used this technique to identify distinct subsets of septin complexes in native and manipulated K562 (Figure 3), a myeloid cell type previously shown to express significant levels of SEPT2, SEPT5, SEPT6, SEPT7, SEPT8, and SEPT11, as well as three of the six confirmed SEPT9 isoforms (Figure 1B; Sellin *et al.*, 2011b, 2012). The data shown in Figure 3 are based on detection of ubiquitously expressed representatives of each one of the four septin subgroups, namely SEPT7, SEPT9, SEPT2, and SEPT6. Analysis of wild-type K562 (Figure 3A) recapitulated previous findings and provides general support for the notion that all heterohexamers and heterooctamers consist of SEPT2 and SEPT6 subgroup members and SEPT7 and that octamers additionally contain SEPT9. The present analysis also detected a minor proportion of SEPT2 and SEPT6 with migration properties consistent with tetrameric and/or dimeric subunit conformations.

To investigate rules governing pairing of septins in K562 cells, we used two general strategies. First, we analyzed septin complexes under conditions in which all endogenous SEPT9 isoforms were replaced by AcGFP-tagged SEPT9(a) (Figure 3B). The expression level of AcGFP-tagged SEPT9(a) was attuned to achieve a stoichiometric (approximately twofold) excess relative to endogenous septins. Figure 3B shows a predominant fraction of AcGFP-SEPT9(a)-containing octamers that migrated as predicted, that is, as a well-resolved complex slightly above complex *i*. Detection of SEPT9 also revealed a minor fraction of AcGFP-SEPT9(a) monomers (marked with #; note that both the N-terminal extension and fusion partner retard the migration of these monomers; see Supplemental Figure S2). Most significantly, the relative proportions of SEPT2, SEPT6, and SEPT7 subunits in hexamers and AcGFP-SEPT9(a)-containing octamers all appeared to be the same. These data support the assumption that octamers and hexamers are all arranged in an analogous subgroup-specific manner and that only octamers may contain SEPT9, which in turn suggests stringent subgroup-restricted hetero-oligomerization.

In a second approach, the heteromeric context of septins in cells lacking SEPT7 or SEPT9 was addressed by analysis of short hairpin RNA (shRNA)–expressing cell lines. Figure 3C shows the heteromer composition of SEPT9-depleted cells. The data reveal that upon depletion of SEPT9, essentially all of SEPT2, SEPT6, and SEPT7 exist as subunits of heterohexamers. Analysis by SDS–PAGE and quantitative Western blotting showed that SEPT9 depletion did not detectably alter the amounts of other septins (Figure 3D).

SEPT7 depletion of various cell types has been shown to reduce the stability of other septin family members (Kinoshita *et al.*, 2002; Estey *et al.*, 2010; Sellin *et al.*, 2011b), which was confirmed by SDS–PAGE and quantitative Western blotting of SEPT7-depleted K562 cells (Figure 3F). Blue native PAGE analysis of the residual septins showed that SEPT2 and SEPT6 only exist as heterodimers and heterotetramers in the absence of SEPT7 (Figure 3E), which is as predicted by previous reports (Sellin *et al.*, 2011b; Kim *et al.*, 2012). Residual SEPT9 in SEPT7-depleted cells was poorly recovered during separation by blue native PAGE and was not discernible in Figure 3E. Nevertheless, all residual SEPT9 isoforms existed as monomers in the absence of available SEPT7 (Supplemental Table S1 and Supplemental Figure S2). Figure 3G summarizes the heteromeric septin complexes detected in wild-type and specifically depleted K562 cells.

The high resolution achieved with blue native PAGE strengthens and extends previous conclusions concerning core heteromer pools in K562 cells (Sellin *et al.*, 2011b). Thus the results verify that SEPT7, which is the sole member of its subgroup (Figure 1A), is essential for assembly of SEPT2 and SEPT6 subgroup members into stable and uniform heteromers. In addition, under all conditions, there is an apparent strict requirement for SEPT7 in assembly of SEPT9 into complexes containing SEPT2 and SEPT6 subgroup members, which is in accordance with the predicted pairing of SEPT9 with SEPT7 at heterooctamer ends as depicted in Figure 1A. These results support the notion that all naturally occurring septin heteromers are arranged according to the homology subgroup membership of subunits.

Lymphocytes are distinguished by prevalent octameric and tetrameric septin heteromers

Because SEPT7 and SEPT9 appear to be expressed in all tissues but the composition of specific SEPT9 isoforms is variable, we next performed a similar analysis of septin composition in a variety of cell types. Analysis by SDS–PAGE and Western blotting in Figure 4A revealed similar levels of SEPT7 in representatives of epithelial, myeloid, and lymphoid cell types. It is also evident that SEPT9 isoforms varied among these cell types and that lymphocytes, such as B-blasts, primary T-blasts, and Jurkat T-blastoid leukemia, mainly expressed the smallest isoform, SEPT9(f). The estimated SEPT7-to-SEPT9 ratio in the cells analyzed was fairly similar, but this ratio was generally higher among lymphocytes (Figure 4A, bottom; the ratio in Jurkat cells is arbitrarily set as 1).

Blue native PAGE analysis showed that K562, HeLa, and HEK 293 cells all have a similar hexamer-to-octamer ratio, whereas lymphocytes have distinctively low hexamer content (compare Figure 4B, top and bottom). Moreover, only octamer complex *iii* was detected in B-blasts, which agrees with the finding that SEPT9(f) is the sole isoform detected by Western blot. Also in accordance with our present assignment of heterooctamer subsets (Figure 1D), the proportions of complexes *i*–*iii* in T-blasts and Jurkat cells are as would be anticipated from their SEPT9 isoform composition.

Immunodetection of SEPT7 highlights that the proportion of heterohexamers varies among cell types and is particularly low in lymphocytes (Figure 4B, bottom). Although the data revealed the anticipated inverse correlation with SEPT9:SEPT7 ratio (compare Figure 4, A and B), this analysis also revealed that lymphocytes are distinguished by complexes migrating slightly above the 4-mer marker (i.e., the recombinant SEPT2-SEPT6 heterotetramer; Supplemental Figure S1). These apparent tetramers were readily detected by both anti-SEPT7 and anti-SEPT9 in Jurkat cells. B-blasts and T-blasts have fewer of these complexes, and detection by anti-SEPT9 required increased exposure times such that the display of octamer subsets became blurred (compare Figure 4 and Supplemental Figure S4).

Assembly of atypical tetramers in lymphocytes depends on both SEPT7 and SEPT9

The T-blastoid Jurkat cell line expresses significant levels of each one of the septin paralogues expressed by myeloid K562 cells, but

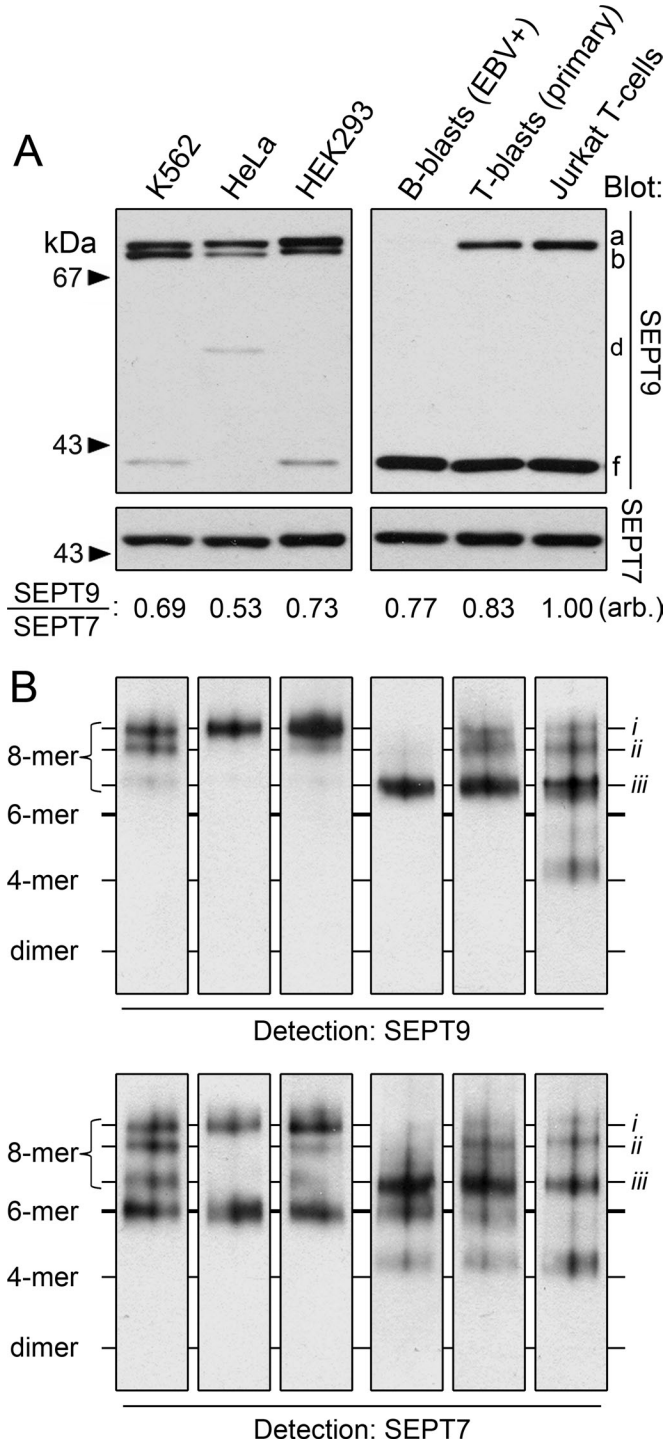

FIGURE 4: SEPT9 isoform and septin heteromer compositions of representatives of epithelial, myeloid, and lymphoid cell types. (A) SEPT9 and SEPT7 content in the indicated cells was analyzed by SDS–PAGE and Western blotting as in Figure 2A. Right, positions of SEPT9 isoforms a, b, d, and f. Isoform c (transcript _*v3*), which may comigrate with isoform b, is not indicated. (B) Septin heteromers as resolved by blue native PAGE followed by detection of SEPT9 (top) and SEPT7 (bottom). Septin complexes are annotated according to Figure 1. The data are representative of three independent analyses.

in addition to a high level of the SEPT9(f) isoform (Figure 4A), Jurkat also expresses SEPT1 and notably high levels of SEPT6 (Sellin *et al.*, 2011b). Because of the unanticipated detection of heterotetramers in Jurkat (and other lymphoid cell types), we subjected Jurkat cells to a similar analysis as performed for K562 by analyzing complexes from wild-type cells and counterparts persistently depleted of SEPT9 or SEPT7.

Blue native PAGE analysis of wild-type Jurkat (Figure 5A) indicated that each of the subgroup representatives exists mainly as subunits in either octamer complex *i* or tetramers migrating slightly above the 4-mer marker. Similar to octamers, tetramers were detected by antibodies against each of the septin homology subgroup representatives. This tetramer category is sufficiently well resolved to be distinguished from the SEPT2–SEPT6 tetramers that accumulate in SEPT7-depleted Jurkat cells (Figure 5, A and C; Supplemental Figure S5 shows a side-by-side comparison).

Blue native PAGE analysis of Jurkat cells persistently depleted of SEPT9 or SEPT7 revealed that, similar to the case for heterooctamers, both SEPT9 and SEPT7 were required for assembly of the heterotetramer subset identified in lymphocytes. Thus each of the subgroup representatives existed almost exclusively as subunits of heterohexamers in SEPT9-deficient cells (Figure 5B), whereas residual SEPT2 and SEPT6 in SEPT7-deficient Jurkat cells existed as tetramers migrating as the 4-mer marker (Figure 5C). Residual SEPT9 was below the detection limit of blue native PAGE. However, analysis of hydrodynamic parameters confirmed that residual SEPT9 was present as monomers in SEPT7-deficient Jurkat cells (Supplemental Table S1).

Our analyses of K562 cells (Figure 3) and Jurkat cells (Figure 5 and Supplemental Figure S5) are consistent with respect to a strict requirement for SEPT7 in order for SEPT9 to form hetero-oligomers with other septins. These findings support the notion that all naturally occurring septin heteromers are arranged according to homology subgroups. However, this comparative analysis also revealed clear-cut differences between cell types with respect to formation of a category of heterotetramers that are detected by antibodies against each one the four homology subgroups. This tetramer category could also be detected in primary lymphocytes (Figure 4 and Supplemental Figure S4A).

Evidence detailed in relation to Supplemental Figure S5 indicates that heterotetramers in lymphocytes represent authentic protomer units of septin filaments. These tetramers were detected by antibodies against each one of the septin subgroup representatives, which provide the basis for the designation "atypical tetramers." It is notable that excessive SEPT9(e) and SEPT9(f) levels in transfected K562 cells results in a minute but still detectable fraction of atypical tetramers and that tetramers containing either of these isoforms can be distinguished by blue native PAGE (Supplemental Figure S2). These data, combined with the evidence for obligate subgroup-restricted septin–septin pairing, suggest that atypical tetramers in lymphocytes are arranged as one-half of an octameric unit (depicted in Figure 5D).

SEPT3-homology subgroup members are replaceable but not equivalent

We next undertook examination of specific properties of individual members of the SEPT3 subgroup (SEPT3, SEPT9, and SET12), which all exhibit differences. For example, the evolutionary rate of SEPT12 is higher than that of other SEPT3 subgroup members (Cao *et al.*, 2007). In addition, only neural cells contain detectable SEPT3, and only sperms contain detectable SEPT12 (Tsang *et al.*, 2011). These two SEPT3 subgroup members both lack an N-terminal extension, which means that they are most similar to the smallest of all SEPT9 isoforms, SEPT9(f).

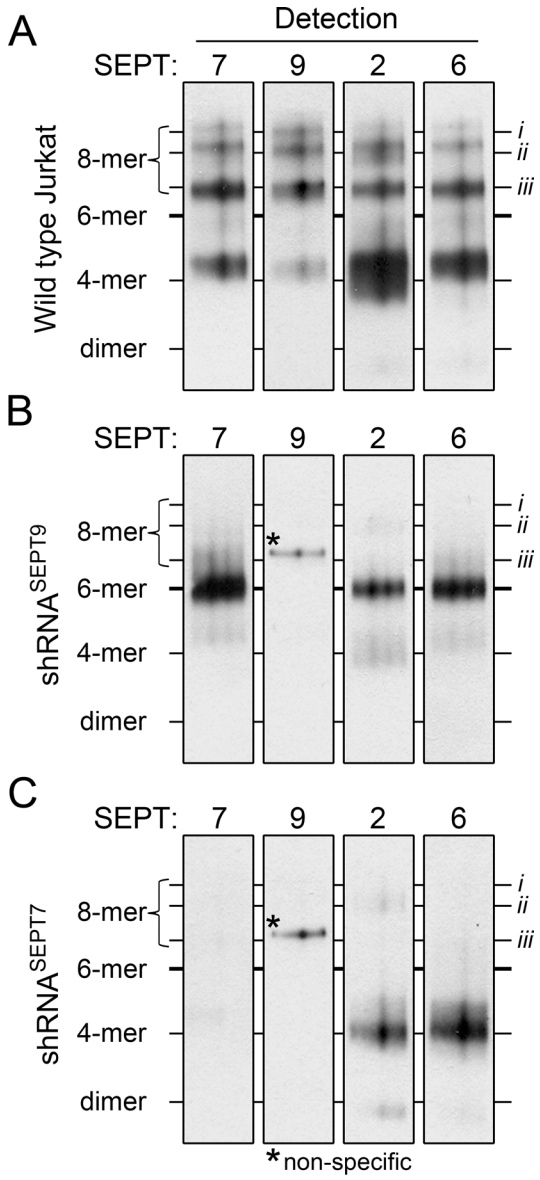

D

Wild type Jurkat, 8-mer:
9(a/f)-**7**-**6**s.gr-**2**s.gr-**2**s.gr-**6**s.gr-**7**-**9**(a/f)

4-mer:
9(f)-**7**-**6**s.gr-**2**s.gr

SEPT9-depleted, 6-mer:
7-**6**s.gr-**2**s.gr-**2**s.gr-**6**s.gr-**7**

SEPT7-depleted, 4-mer:
6s.gr-**2**s.gr-**2**s.gr-**6**s.gr

FIGURE 5: Subunit composition of heteromers with a specified number of subunits in control and genetically manipulated Jurkat T-blastoid cell lines. (A) Septin heteromers of normal Jurkat cells were resolved by blue native PAGE, followed by immunodetection of the septin homology subgroup representatives indicated. Septin complexes are annotated according to Figure 1. (B) SEPT9-depleted Jurkat cells were analyzed as in A. Cell lines expressing shRNA^{SEPT9} were generated by the same general protocol as in Figure 1C. Similar to the corresponding analysis of K562 cells in Figure 2, detection of SEPT9 revealed a nonspecific band (indicated by asterisk) after prolonged exposure. (C) SEPT7-depleted Jurkat cells were analyzed as in A. Transfected cell lines expressing shRNA^{SEPT7} were generated according to the same general protocol as in B. Prolonged exposure revealed the same cross-reactive band as in B (indicated by asterisk). (D) Septin heteromers in wild-type and specifically depleted Jurkat cells are depicted according to premises described in Figure 3G. Atypical tetramers are depicted to be arranged according to homology subgroup membership (s.gr). The data are representative for Jurkat cell lines derived from two independent transfections.

To investigate SEPT3 subgroup–specific properties in a given cell type, we constructed pMEP expression derivatives with coding sequence of SEPT3 or SEPT12 fused to codons for the Flag-epitope tag. To minimize effects on the level of transcript, we placed coding sequences so that the open reading frames were surrounded by the same 5′ and 3′ sequences as the cognate SEPT9 derivative. K562 cells expressing these derivatives were analyzed by SDS–PAGE and Western blotting, which revealed that anti-SEPT9 detected ectopic expression of Flag-SEPT3 but not expression of Flag-SEPT12 (Figure 6A). Based on cross-reactivity of anti-SEPT9, the data suggest similar or higher levels of Flag-SEPT3 than SEPT9(f). However, Flag-SEPT12 appears to be intrinsically unstable in K562 cells, and detection by anti-Flag suggested a level that was approximately fourfold to eightfold lower than that of Flag-SEPT3.

Highly expressed ectopic SEPT9 reduces the amount of endogenous SEPT9, which can be attributed to competition for a limiting number of appropriate stabilizing hetero-oligomerization partners (Sellin *et al.*, 2012). The Western blots shown in Figure 6A confirmed that ectopic SEPT9(f) caused a decrease in endogenous SEPT9(a) and SEPT9(b) isoforms. Of importance, Flag-SEPT3 caused a similar reduction in all three SEPT9 isoforms. Such a decrease was not evident in Flag-SEPT12–transfected cells, but this is readily explained by the low level of the Flag-SEPT12 protein. These data provide suggestive evidence that there may be competition among SEPT3 subgroup members for common hetero-oligomerization partners.

Blue native PAGE analysis showed that both Flag-SEPT3 and Flag-SEPT12 may serve as heterooctamer subunits (Figure 6B), since detection of the Flag epitope (top) revealed octamers that migrated close to complex *iii*. In addition, a subset of Flag-SEPT3–containing octamers that migrate close to complex *ii* was also clearly distinguishable, which suggests the presence of octamers containing SEPT3 at one end and endogenous SEPT9(a) or SEPT9(b) at their other end (see the assignment of complexes *i*–*iii*, Figure 1). Of interest, Flag epitope and SEPT7 detection in Figure 6B revealed generation of tetramers and corresponding reduction of hexamers. Under the same conditions, ectopic SEPT9(f) generated predominantly octamers. Quantification of SEPT7-containing heteromer complexes reveals only a minor fraction of tetramers in SEPT9(f)-expressing cells as compared with cells expressing SEPT3 or SEPT12 (Figure 6C). Thus all members of the SEPT3 subgroup may participate in the assembly of both heterooctamers and heterotetramers, but with notably different propensities.

It can be deduced from the present data that modest levels of the evidently unstable Flag-SEPT12 protein severely reduced the hexamer content, which was associated with a corresponding increase of tetramers. As anticipated from the analysis of naturally occurring atypical tetramers in lymphocytes (Supplemental Figure S4 and Figure 5), tetramers generated in transfected K562 cells could also be detected by antibodies against SEPT2 and SEPT6 subgroup members (unpublished observations). This suggests that tetramers

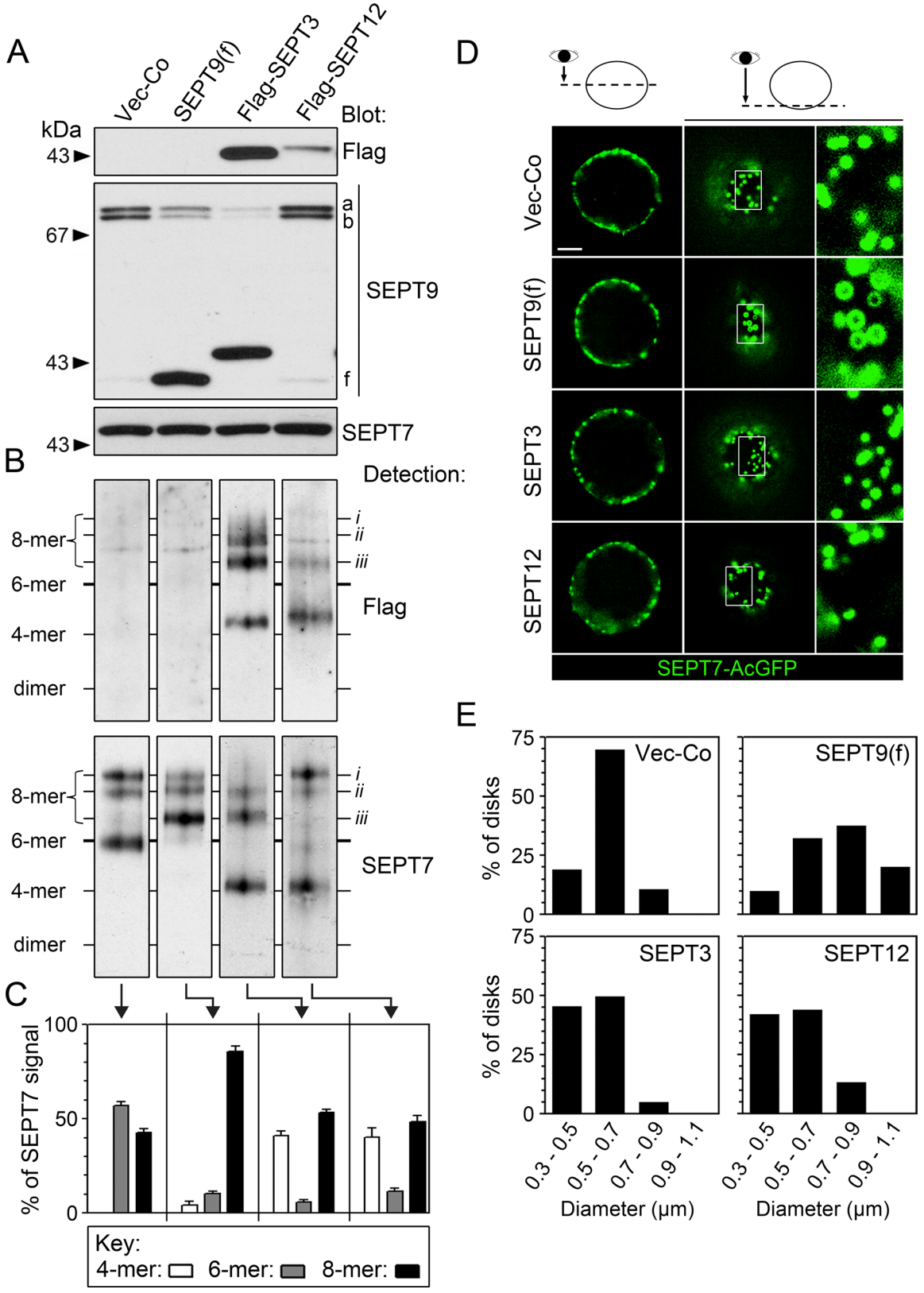

FIGURE 6: SEPT9 content and subunit number of heteromers in K562 cells expressing ectopic SEPT3-subgroup members. K562 cells were transfected with empty vector (Vec-Co) or the indicated pMEP derivatives of each member of the SEPT3 subgroup, followed by counterselected with hygromycin for ~1 wk. The conditions for constitutive expression from the hMTIIa promoter were the same as in Figure 1C. (A) SDS–PAGE followed by Western blot detection of Flag epitope–tagged SEPT3 and SEPT12, and of SEPT9 and SEPT7. Right, positions of endogenous SEPT9 isoforms a, b, and f. (B) Septin heteromers as resolved by blue native PAGE, followed by detection of the Flag epitope tag (top) and SEPT7 (bottom). Septin complexes are annotated according to Figure 5. (C) Proportions of tetrameric, hexameric,

in SEPT3- and SEPT12-expressing K562 cell lines are arranged according to homology-subgroup membership of subunits, as depicted in Supplemental Table S2.

Similar to the SEPT9(f) isoform, SEPT3 and SEPT12 have also only short sequences flanking either side of the G domain. Structural data are consistent with the idea that these septins may function as equivalent G domains within a given heteromeric context (Macedo *et al.*, 2013). Hence ectopic expression of SEPT9(f), SEPT3, and SEPT12 in K562 cells may reveal how differential proportions of heterooctamers, heterohexamer, and heterotetramers influence higher-order septin assemblies. To perform this type of analysis, we used a system that relies on replacement of endogenous SEPT7 with SEPT7-AcGFP (Sellin *et al.*, 2011a). To ascertain that SEPT7-AcGFP levels are unaltered in the presence of ectopic SEPT3 subgroup members, we analyzed transfected cell lines by flow cytometry, which indicated similar fluorescence intensities as Vector-Co cells (Supplemental Figure S6). As evidenced by cell images presented in Figure 6D, none of the SEPT3 subgroup members alter the general localization of SEPT7-AcGFP, which in all cases visualized previously described circular structures along the plasma membrane (images represent optical sections at the cell equator and parallel to the plasma membrane).

The structures visualized by SEPT7-AcGFP in Figure 6D—which we refer to as septin disks—represent the prevalent interphase arrangement in substrate-independent spherical cell types (Sellin *et al.*, 2011a). Figure 6E shows that SEPT3 subgroup members exert differential effects on the size distribution of these septin disks. Consistent with our previous report (Sellin *et al.*, 2012), comparison between Vector-Co and SEPT9(f)-overexpressing cells shows that an increased proportion of octamers increases the average size of septin disks. Of importance, expression of SEPT3 or SEPT12, which results in replacement of hexamers with tetramers (Figure 6C), alters the size distribution such that the average is decreased.

Our previous study showed that SEPT9 depletion of K562 cells causes a decreased average size of septin disks (Sellin *et al.*, 2012), which is in line with the present results. It seems plausible that two atypical tetramers (arranged as depicted in Supplemental Table S2) may replace an octamer in apolar septin filaments. Such an increased proportion of tetramers can be envisaged to decrease the stability of septin filaments and thereby decrease the average size of circular structures such as septin disks. This would explain why ectopic SEPT9(f) causes an increased sizes range, whereas SEPT3 and SEPT12 have the opposite effect (Figure 6).

Neural cells contain heterotetramers and heterooctamers, but hexamers are nonprevalent

To evaluate the significance of findings based on genetically manipulated cell lines, we analyzed native core heteromers in brain tissue, which contains SEPT3 and SEPT9 but not SEPT12 (http://mouse.brain-map.org/). Figure 7A shows analysis by SDS–PAGE and Western blotting of tissue derived from different parts of mouse brain. As a reference, a K562 extract was coanalyzed. Loadings were adjusted according to SEPT7 content (5 µg of brain tissue/lane; 20 µg of K562/lane). The data revealed two SEPT7 isoforms and confirmed that SEPT3 is expressed in brain tissues but not in K562 cells. SEPT3 blots of brain also revealed two minor bands (~52 and ~56 kDa), which may suggest either cross-reactivity or previously unrecognized larger isoforms. Interpretation of the SEPT9 blot is potentially flawed by cross-reactivity with native mouse SEPT3, which comigrates with SEPT9(f). Nevertheless, it still appears clear that the large SEPT9 isoforms are rare (e.g., cerebrum and olfactory bulb samples) or nonexistent (e.g., cerebellum).

Blue native PAGE analysis combined with SEPT3 detection (Figure 7B) revealed some differences between brain tissues, but in all cases octamers migrating similarly to complex *iii* were detectable. Of note, tetramers migrating similarly to the atypical tetramers of lymphocytes were also readily detected. Detection of SEPT9, which under the conditions used for blue native PAGE seemed less flawed by cross-reactive detection of SEPT3, barely detected any heterotetramers but revealed a dominant octamer—complex *iii* (Figure 7B)—consistent with a predominant SEPT9(f) isoform. Detection of SEPT7—a predicted obligatory hetero-oligomerization partner of SEPT3 subgroup members—revealed relatively poorly resolved octamers in brain tissues (Figure 7B), which may be attributed to heterogeneity among cells with differentially expressed SEPT3 and SEPT9. Even so, SEPT7 detection did reveal heterotetramers in all brain tissue samples, whereas hexameric heteromers are, by and large, only evident in olfactory bulb tissue.

It is notable that the atypical tetramers in brain tissue have low SEPT9 content. Furthermore, brain-derived tetramers were also revealed by detection of SEPT2 and SEPT6 (unpublished observations). These results fulfill predictions based on analysis of atypical tetramers in genetically manipulated cell lines. Given the evidence for obligatory subgroup-restricted septin–septin pairing, the present study suggests that atypical tetramers in neural tissues are arranged as one-half of an octameric building block that contains mainly SEPT3 at one end. Taken together, the present results suggest that the predominant building blocks for septin filaments in brain are composed as depicted in Figure 7C (note that hexamers are only detected in the olfactory bulb).

DISCUSSION

In this study, we validated a method for identification of subsets of septis heteromers. When used in combination with wild-type and genetically manipulated cells, this method allowed us to address a previously recalcitrant question—namely, the heteromeric context of mammalian septin paralogues in diverse cell types. The results confirm, and significantly extend, our knowledge of the functional significance of the four homology-based septin subgroups that are conserved among chordates but not other phyla. Our data also

and octameric septin complexes were determined by blue native PAGE separation, followed by detection of SEPT7. Quantification was performed by serial dilution of cell lysates, with the relative amounts calculated from a standard curve. A representation of the predominant septin heteromers in K562 cells transfected with SEPT9(f), SEPT3, or SEPT12 is shown in Supplemental Table S2. (D) Epifluorescence microscopy of live K562 cells in which heteromers are visualized by replacement of endogenous SEPT7 with SEPT7-AcGFP. Images of representative cells expressing the indicated pMEP derivatives are shown. They represent deconvoluted optical sections at either the equatorial plane or parallel to the plasma membrane, as indicated at the top (note that K562 cells have a spherical shape). The distribution of the total fluorescence intensity among cells is shown in Supplemental Figure S6. Scale bar, 5 µm. (E) Size distribution of SEPT7-AcGFP–visualized disk-like structures in K562 cells expressing the indicated pMEP derivatives (Vector-Co, $N = 288$; SEPT9(f), $N = 210$; Flag-SEPT3, $N = 216$; Flag-SEPT12, $N = 231$). The data are representative for cells lines derived from two or more transfections, which were analyzed on at least four occasions.

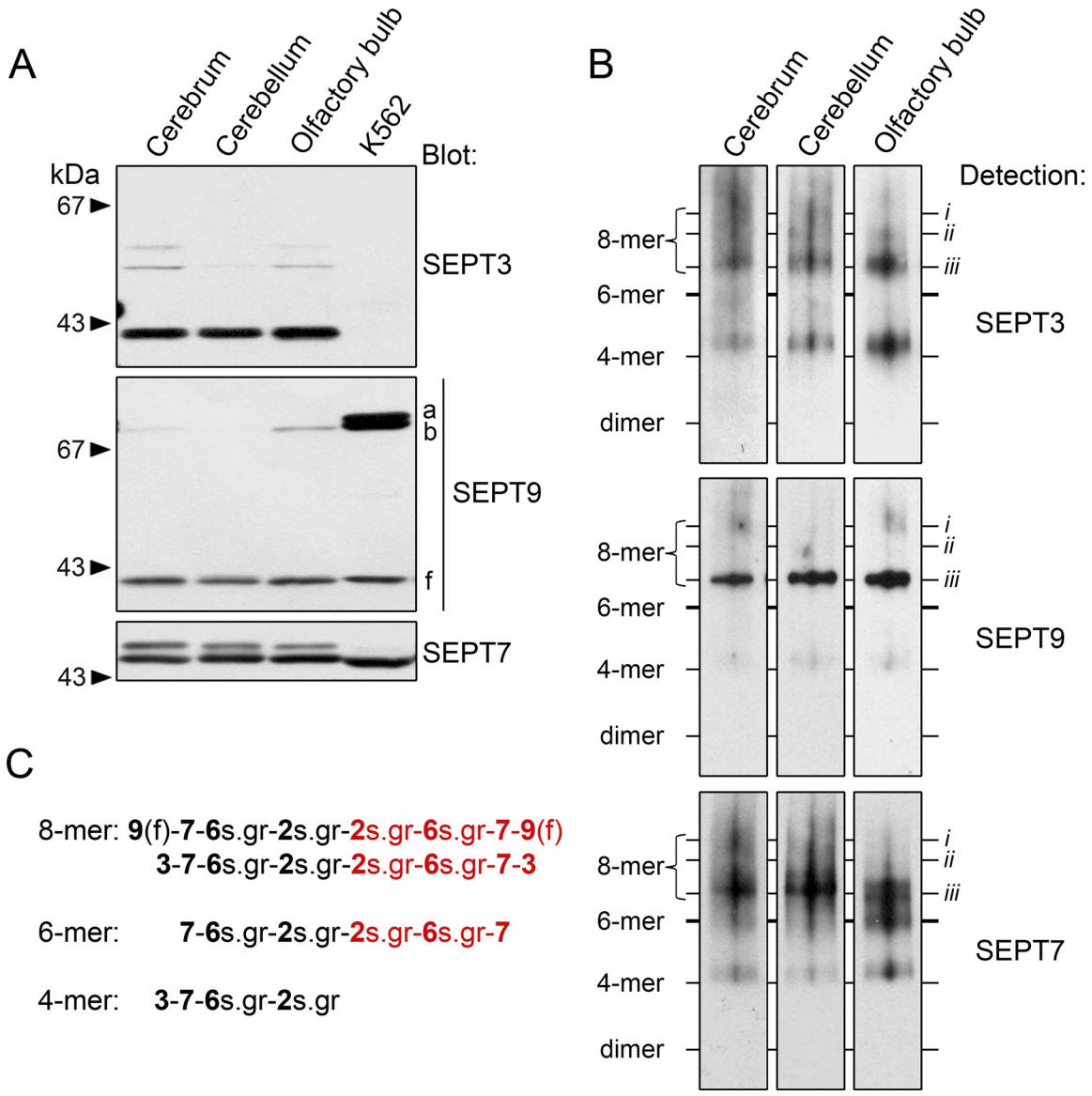

FIGURE 7: Septin expression and the subunit number of heteromers in brain tissues. (A) SEPT3, SEPT9, and SEPT7 expression in the indicated parts of mouse brain was analyzed by SDS–PAGE and Western blotting (loaded at 5 µg/lane). As a reference, the analysis also included the human cell line K562 (loaded at 20 µg/lane). Right, positions of isoforms a, b, and f. (B) Septin heteromers as resolved by blue native PAGE, followed by detection of SEPT9 (top) and SEPT7 (bottom). Septin complexes are annotated according to Figure 5. (C) Septin heteromers in brain-derived tissues are depicted according to premises stated in Figure 3G. Atypical tetramers, which are depicted to be arranged according to homology subgroup membership, contain mainly a single SEPT3 subgroup member, namely SEPT3. Note that only the olfactory bulb contains detectable amounts of hexamers. The data are representative of three independent analyses.

revealed unexpected features of SEPT3 subgroup members that affect the relative ratio of septin heterotetramers, heterohexamers, and heterooctamers present, which ultimately influence aspects of higher-order filamentous assemblies. These results provide a first glimpse of determinants that direct the assembly of cell type–specific pools of core heteromers.

SEPT3 subgroup–specific properties

Orthologues of the SEPT3 homology–based subgroup (SEPT3, SEPT9, and SEPT12) exist only in vertebrates. Gene targeting in mice revealed no essential role of SEPT3 (Tsang *et al.*, 2008) but showed that SEPT9 is essential during embryonic development (Fuchtbauer *et al.*, 2011) and SEPT12 is specifically required for the functioning of sperm (Lin *et al.*, 2009). Moreover, tissue-specific SEPT9 isoforms modulate higher-order septin structures (Sellin *et al.*, 2012; Bai *et al.*, 2013). Although the function of SEPT3 appears redundant in mice, these reports are all consistent with the idea that individual SEPT3 subgroup members (and isoforms) have cell type–specific functions.

It was recently demonstrated that recombinant SEPT3 forms soluble homo-oligomers of various sizes, but an N-terminally truncated version lacking the α0 helix, which is located within the N-C interface of the G domain, is monomeric (Macedo *et al.*, 2013). Our studies showed that all isoforms of SEPT9 exist solely as monomers

in SEPT7-depleted K562 and Jurkat cells (Supplemental Table S1; Sellin *et al.*, 2011b). If overexpressed threefold to sixfold in K562, SEPT9 exists either as subunits of heterooctamers or as monomers (Supplemental Figure S2B). These findings support the idea that SEPT7 is required for SEPT9 hetero-oligomerization. However, we also found that ~60-fold overexpression results in SEPT9 homo-oligomers of various sizes (Figure 2). These oligomers are soluble and are recovered by a protocol shown to disassemble all native higher-order septin structures into heteromers (Sellin *et al.*, 2011b). We noted that—depending on expression levels—SEPT3 may also either form soluble homo-oligomers or exist as monomers (unpublished data). These findings adhere to subgroup-specific properties as predicted by structural analysis of recombinant SEPT3 (Macedo *et al.*, 2013).

Heterohexamers were originally identified by recombinant coexpression of SEPT2, SEPT6, and SEPT7 (Kinoshita *et al.*, 2002). Within crystals, these heterohexamers are arranged as continuous filaments in which subunits interact through alternating G and N-C interfaces (Figure 1A; Sirajuddin *et al.*, 2007). This arrangement is also evident within crystals of singly expressed constructs of SEPT2 (Sirajuddin *et al.*, 2007), SEPT7 (Zent *et al.*, 2011), and SEPT3 (Macedo *et al.*, 2013). A comparison of homotypic interactions within crystals of SEPT2, SEPT7, and SEPT9 revealed contributions by certain nonconserved residues unique to the SEPT3 subgroup (Macedo *et al.*, 2013). It was concluded that 1) terminal SEPT3 subunits have the potential to mediate end-to-end polymerization of recently identified heterooctamers, and 2) SEPT3 subgroup members are likely to confer equivalent N-C interfaces at hetero-octamer ends.

SEPT3-subgroup members are highly homologous within the G domain, which lacks a C-terminal extension (Cao *et al.*, 2007). Isoform variation is common among mammalian septins, but SEPT9 is exceptional in having isoforms differing almost twofold in mass due to a variable N-terminal extension. In contrast, all known isoforms of SEPT3 and SEPT12 have nonvariable N-termini of a similar length to that of the shortest SEPT9 isoform, SEPT9(f), which has only a 31-residue N-terminal extension from the predicted α0-helix of its G domain. According to arguments based on SEPT3 crystals (Macedo *et al.*, 2013), it may be assumed that SEPT3, SEPT9(f), and SEPT12 function as equivalents within heterooctamers and heterotetramers. Hence, among SEPT3 subgroup members, it seems quite possible that only certain large SEPT9 isoforms would be able to confer specific properties on septin heterooctamers. Furthermore, it follows from our findings that functional differences between the G-domains of SEPT3 subgroup members may be confined to their differential propensity to generate atypical tetrameric building blocks.

SEPT9 depletion of HeLa cells decreases the size of cytosolic circular septin structures that develop soon after disruption of actin filaments by the drug cytochalasin (Kim *et al.*, 2011). In apparent analogy, we found that SEPT9 depletion of K562, which transforms a mixed pool of octamers and hexamers into a uniform pool of hexamers, decreases the size of submembranous septin disks, which represent a prevalent structure in substrate-independent cell types (Sellin *et al.*, 2012). It is notable that HeLa and K562 cells have a similar octamer-to-hexamer ratio (~1:1, Figure 4) and that SEPT9 depletion of these two cell types results in a similar degree of decreased size range of circular but otherwise distinct kinds of septin structures.

Consistent with our previous report (Sellin *et al.*, 2012), the only discernible effect of manipulating the proportions of heteromer categories was an altered size range of septin disks (Figure 6). These results suggest that heterooctamers, heterohexamers, and heterotetramers may polymerize into common filamentous structures. Along these lines, it seems possible that two atypical heteromers may replace one octamer, but interaction cooperativity may decrease if each building block contains only half the number of subunits. Hence an increased structural stability of filaments provides a simple explanation for a positive correlation between the subunit number of heteromers and size range of septin disks shown in Figure 6. This would also explain the corresponding size alterations, which were linked to changes in the octamer-to-hexamer ratio in control and SEPT9-depleted cells (Sellin *et al.*, 2012).

Assembly and composition of cell type–specific pools of septin heteromers

The present article substantiates previous evidence for subgroup-restricted assembly of two discrete heteromer categories, namely heterohexamers and heterooctamers, which are present in similar proportions in K562, HeLa, and HEK293 cells (Figure 4). In addition, an unanticipated cell type–restricted category of atypical tetramers was identified. The evidence that these tetramers represent authentic building blocks of septin filaments relies on analyses of live cells (Figure 6) and scoring of decay products of native octamers and hexamer (outlined in relation to Supplemental Figure S5; Sellin *et al.*, 2011a,b).

The high resolutions by which heteromer subpopulations are resolved by blue native PAGE substantiate previous evidence of cooperativity during heteromer assembly. Thus all of the septin complexes detected consist of two, four, six, or eight subunits. Moreover, replacement of endogenous SEPT9 isoforms in K562 cells by a single large SEPT9 isoform (expressed at substoichiometric levels) revealed well-resolved heterohexamers and heterooctamers but no heptamers (Figure 1). Thus, although it is difficult to envision cooperative interactions between terminal subunits, our data point to an assembly process that in some way ensures stable heteromeric building blocks. This appears to be of particular significance during octamer assembly, which in several cell types is restrained by limiting amounts of SEPT9 (Figure 4; Sellin *et al.*, 2011b, 2012).

Analyses of recombinant septin complexes by x-ray crystallography and electron microscopy led to the current paradigm of uniform pairing within apolar building blocks of apolar septin filaments (John *et al.*, 2007; Sirajuddin *et al.*, 2007; Bertin *et al.*, 2008). Whereas a mammalian heterooctamer may have different SEPT9 isoforms at each end (Figure 1), the general aspects of this paradigm are still reinforced by our evidence that all native septin complexes have an even number of subunits. Here we have now shown that hexamers are rare in lymphocytes and neural cells, which are distinguished by their predominant pool of heterooctamers and a previously unanticipated category of atypical tetramers. As discussed here, analysis of live cells in Figure 6 suggests that these tetramers polymerize into the same type of apolar filaments as hexamers and octamers but may cause decreased stability of higher-order septin structures.

As evidenced in shRNA-expressing K562 and Jurkat cells (Figure 5), expression of SEPT7 is strictly required for hetero-oligomerization of SEPT9. Furthermore, analysis of heteromers in transfected K562 cells shows that the cell context is important for SEPT9-dependent generation of hetero-tetramers and that a stoichiometric excess of SEPT9 does not generate tetramers by default (Figure 1B, Supplemental Figure S2A, and Figure 6C). The T-blastoid Jurkat cell line expressed significant levels of each of the septin paralogues expressed by myeloid K562 cells, but in addition to notably high levels of SEPT9(f) and SEPT6, Jurkat cells also express the SEPT2 subgroup member SEPT1 (Sellin *et al.*, 2011b), which appears restricted to lymphocytes (Cao *et al.*, 2007). However, the relevance of these

qualitative and quantitative differences in available septin subunits remains to be established.

Concluding remarks

Alternative hetero-oligomers and cell type–/differentiation stage–specific expression of septins are not restricted to animal cells. For example, there is biochemical and genetic evidence for alternative terminal subunits of heterooctamers in budding yeast (Garcia *et al.*, 2011). Furthermore, certain septin paralogues in yeast organisms are differentially expressed during mitotic and meiotic division (reviewed in McMurray and Thorner, 2009).

It was recently reported that septins in *Drosophila* are specifically needed to disengage contacts with neighboring cells during planar cytokinesis but are dispensable for cell types that divide perpendicular to the plane of a single-layered epithelium (Founounou *et al.*, 2013). This provides an example of a cell type–specific septin function that also appears to be relevant for mammals, since depletion/mutational inactivation of septins affects division of epithelial and fibroblastic cells (Estey *et al.*, 2010; Fuchtbauer *et al.*, 2011), whereas cells that grow in suspension—such as K562 or Jurkat—appear to be unaffected (unpublished observations). Along these lines, phenotypes of septin-null mutants are disparate among yeast organisms (for references, see Wu *et al.*, 2010). Thus both fungal and animal model systems indicate cell type–specific functions, which in some cases involve specific septin paralogues. Future analysis of the native pools of heteromeric septin complexes in various organisms may reveal that some of the presently identified SEPT3 subgroup–restricted properties are conserved.

MATERIALS AND METHODS

Shuttle vector DNA constructs, regulatable ectopic expression, gene product replacement, and generation of transfected cell lines

Construction of the EBV-based shuttle vector, denoted shRNA^{SEPT9}, which directs constitutive expression of shRNA targeting mRNAs encoding all confirmed SEPT9 isoforms through sequences located within the G domain, has been described (Sellin *et al.*, 2012). EBV-based pMEP4 shuttle vectors directing regulatable expression of septins are described in the Supplemental Materials and Methods. Transfection of human lymphoblastoid Jurkat cells and myeloid K562 cells with shuttle vectors and selection of hygromycin-resistant cell lines was as previously described (Holmfeldt *et al.*, 2007). The conditions for constitutive and inducible expression from the hMTIIa promoter were as described in Sellin *et al.* (2011a). Cell lines persistently depleted of SEPT7 or SEPT9 by RNA interference were generated by transfection of EBV-based shuttle vectors directing expression of shRNA as previously described (Sellin *et al.*, 2011b). For replacement of endogenous SEPT9 with single SEPT9 isoforms, cells were transfected with a mixture of 2 µg of shRNA^{SEPT9}, 4 µg of the indicated pMEP-SEPT9 derivative (which is shRNA^{SEPT9} resistant), and empty pMEP4 vector up to a total of 16 µg of DNA. A previous study confirmed stringent replication control of the EBV-based vectors—for example, that the ratio of transfected DNAs remains similar for several weeks (Melander Gradin *et al.*, 1997).

Preparation of extracts for analysis of cellular pools of septin heteromers

The rationale behind the present protocol for preparing cell extracts is based on the finding that native septin filaments in a variety of human cell types are effectively disassembled into soluble components upon cell permeabilization in a buffer originally designed to preserve tubulin heterodimers (Sellin *et al.*, 2011a,b). Accordingly, cells were permeabilized on ice by 0.2% saponin in a buffer composed of 80 mM 1,4-piperazinediethanesulfonic acid (pH 6.8), 5 mM $MgCl_2$, 4 mM ethylene glycol tetraacetic acid, 0.1 mM guanosine 5′-triphosphate, 25 mM ε-aminocapric acid, 10 µg/ml leupeptin, and 10 µg/ml Pefabloc. The volume of permeabilization buffer was adjusted to yield a final concentration of 3–6 mg/ml soluble protein. For homogenization of tissues, a rotating piston was used. Extracts were clarified by centrifugation (20 min, 14,000 × *g*). To achieve complete disassembly of septin structures into protomer units, NaCl (0.45 M final concentration) was added to the supernatant. After a second round of centrifugation (10 min, 14,000 × *g*), extracts were passed over a desalting column (30-kDa cutoff; Micro Bio-Spin P30 Column; Bio-Rad, Hercules, CA) that was equilibrated in 40 mM BisTris-HCl (pH 7.2) containing 0.3 M NaCl, 1 mM ethylene glycol tetraacetic acid, 25 mM ε-aminocapric acid, and 0.2 mM $MgCl_2$. Recovered proteins were mixed with glycerol (50% final concentration) and stored at –20°C until analyzed. Western blot analysis of pelleted material indicated that >90% of all septins was recovered by the present protocol.

Determination of the subunit composition of heteromers with a specified number of subunits

Cell extracts (prepared as described) were diluted to a concentration of 0.4 µg/µl in 50 mM BisTris-HCl (pH 7.2) containing 50 mM NaCl, 6% sucrose, 0.05% Coomassie blue G250, and 250 mM aminocapric acid. For separation of native complexes by blue native PAGE, 4–16% Novex NativePAGE Bis-Tris Gel System precast polyacrylamide gels (Invitrogen, Carlsbad, CA) were loaded with 20 µl/well and run under electrophoresis conditions set according to the recommendations of the manufacturer. For immunodetection, proteins were transferred to polyvinylidene fluoride membranes (100 mA for 18 h) using a nondenaturing transfer buffer containing 31 mM Tris-HCl and 300 mM glycine. Filters were subsequently rinsed in water (10 min), stained with 0.05% Coomassie blue R250 in 50% methanol (0.5 min), and destained (as well as fixed) in 50% methanol containing 10% acetic acid (3 min). Blocking and immunodetection of septin complexes was performed according the same general protocols described for standard Western blot analysis. For probing of filters with consecutive antibodies, filters were stripped in 60 mM Tris-HCl (pH 6.8) containing 0.5% SDS and 100 mM 2-mercaptoethanol (60°C, 15 min).

Western blot analysis, antibodies, and fluorescence microscopy

Cell extracts prepared as described were analyzed by Western blot and subsequent detection using enhanced chemiluminescence as described (Sellin *et al.*, 2011b). Quantification by Western blot was performed by serial dilution of cell lysates, with the relative amounts calculated from a standard curve. Antibodies used for detection of SEPT2, SEPT6, SEPT7, and SEPT9 were as described in Sellin *et al.* (2011b), and detection of SEPT3 was performed using affinity-purified rabbit antibodies (PA5-31124; Thermo Fisher Scientific, Waltham, MA). Septin assemblies were scored by fluorescence microscopy of live SEPT7-AcGFP–expressing cells according to previously described criteria (Sellin *et al.*, 2011a, 2012).

ACKNOWLEDGMENTS

We thank Staffan Bohm for help with dissection of mouse brains and Victoria Shingler for scrutinizing the manuscript. M.E.S. is supported by a Swedish Research Council International Post-Doc fellowship (Grant 2012-262). This work was supported by the Swedish Research Council (Grant 2011-4970).

REFERENCES

Bai X, Bowen JR, Knox TK, Zhou K, Pendziwiat M, Kuhlenbaumer G, Sindelar CV, Spiliotis ET (2013). Novel septin 9 repeat motifs altered in neuralgic amyotrophy bind and bundle microtubules. J Cell Biol 203, 895–905.

Beise N, Trimble W (2011). Septins at a glance. J Cell Sci 124, 4141–4146.

Bertin A, McMurray MA, Grob P, Park SS, Garcia G 3rd, Patanwala I, Ng HL, Alber T, Thorner J, Nogales E (2008). *Saccharomyces cerevisiae* septins: supramolecular organization of heterooligomers and the mechanism of filament assembly. Proc Natl Acad Sci USA 105, 8274–8279.

Cao L, Ding X, Yu W, Yang X, Shen S, Yu L (2007). Phylogenetic and evolutionary analysis of the septin protein family in metazoan. FEBS Lett 581, 5526–5532.

Estey MP, Di Ciano-Oliveira C, Froese CD, Bejide MT, Trimble WS (2010). Distinct roles of septins in cytokinesis: SEPT9 mediates midbody abscission. J Cell Biol 191, 741–749.

Field CM, al-Awar O, Rosenblatt J, Wong ML, Alberts B, Mitchison TJ (1996). A purified *Drosophila* septin complex forms filaments and exhibits GTPase activity. J Cell Biol 133, 605–616.

Founounou N, Loyer N, Le Borgne R (2013). Septins regulate the contractility of the actomyosin ring to enable adherens junction remodeling during cytokinesis of epithelial cells. Dev Cell 24, 242–255.

Fuchtbauer A, Lassen LB, Jensen AB, Howard J, Quiroga Ade S, Warming S, Sorensen AB, Pedersen FS, Fuchtbauer EM (2011). Septin9 is involved in septin filament formation and cellular stability. Biol Chem 392, 769–777.

Garcia G3rd, Bertin A, Li Z, Song Y, McMurray MA, Thorner J, Nogales E (2011). Subunit-dependent modulation of septin assembly: budding yeast septin Shs1 promotes ring and gauze formation. J Cell Biol 195, 993–1004.

Holmfeldt P, Stenmark S, Gullberg M (2007). Interphase-specific phosphorylation-mediated regulation of tubulin dimer partitioning in human cells. Mol Biol Cell 18, 1909–1917.

Hu Q, Milenkovic L, Jin H, Scott MP, Nachury MV, Spiliotis ET, Nelson WJ (2010). A septin diffusion barrier at the base of the primary cilium maintains ciliary membrane protein distribution. Science 329, 436–439.

Ihara M *et al.* (2005). Cortical organization by the septin cytoskeleton is essential for structural and mechanical integrity of mammalian spermatozoa. Dev Cell 8, 343–352.

John CM *et al.* (2007). The *Caenorhabditis elegans* septin complex is nonpolar. EMBO J 26, 3296–3307.

Kim MS, Froese CD, Estey MP, Trimble WS (2011). SEPT9 occupies the terminal positions in septin octamers and mediates polymerization-dependent functions in abscission. J Cell Biol 195, 815–826.

Kim MS, Froese CD, Xie H, Trimble WS (2012). Uncovering principles that control septin-septin interactions. J Biol Chem 287, 30406–30413.

Kinoshita M (2003). Assembly of mammalian septins. J Biochem 134, 491–496.

Kinoshita M, Field CM, Coughlin ML, Straight AF, Mitchison TJ (2002). Self- and actin-templated assembly of mammalian septins. Dev Cell 3, 791–802.

Kissel H, Georgescu MM, Larisch S, Manova K, Hunnicutt GR, Steller H (2005). The Sept4 septin locus is required for sperm terminal differentiation in mice. Dev Cell 8, 353–364.

Lin YH *et al.* (2009). The expression level of septin12 is critical for spermiogenesis. Am J Pathol 174, 1857–1868.

Macedo JN, Valadares NF, Marques IA, Ferreira FM, Damalio JC, Pereira HM, Garratt RC, Araujo AP (2013). The structure and properties of septin 3: a possible missing link in septin filament formation. Biochem J 450, 95–105.

McMurray MA, Thorner J (2009). Septins: molecular partitioning and the generation of cellular asymmetry. Cell Div 4, 18.

Melander Gradin H, Marklund U, Larsson N, Chatila TA, Gullberg M (1997). Regulation of microtubule dynamics by Ca2+/calmodulin-dependent kinase IV/Gr-dependent phosphorylation of oncoprotein 18. Mol Cell Biol 17, 3459–3467.

Mendoza M, Hyman AA, Glotzer M (2002). GTP binding induces filament assembly of a recombinant septin. Curr Biol 12, 1858–1863.

Mostowy S, Cossart P (2012). Septins: the fourth component of the cytoskeleton. Nat Rev Mol Cell Biol 13, 183–194.

Pan F, Malmberg RL, Momany M (2007). Analysis of septins across kingdoms reveals orthology and new motifs. BMC Evol Biol 7, 103.

Sellin ME, Holmfeldt P, Stenmark S, Gullberg M (2008). Global regulation of the interphase microtubule system by abundantly expressed Op18/stathmin. Mol Biol Cell 19, 2897–2906.

Sellin ME, Holmfeldt P, Stenmark S, Gullberg M (2011a). Microtubules support a disk-like septin arrangement at the plasma membrane of mammalian cells. Mol Biol Cell 22, 4588–4601.

Sellin ME, Sandblad L, Stenmark S, Gullberg M (2011b). Deciphering the rules governing assembly order of mammalian septin complexes. Mol Biol Cell 22, 3152–3164.

Sellin ME, Stenmark S, Gullberg M (2012). Mammalian SEPT9 isoforms direct microtubule-dependent arrangements of septin core heteromers. Mol Biol Cell 23, 4242–4255.

Sheffield PJ, Oliver CJ, Kremer BE, Sheng S, Shao Z, Macara IG (2003). Borg/septin interactions and the assembly of mammalian septin heterodimers, trimers, and filaments. J Biol Chem 278, 3483–3488.

Sirajuddin M, Farkasovsky M, Hauer F, Kuhlmann D, Macara IG, Weyand M, Stark H, Wittinghofer A (2007). Structural insight into filament formation by mammalian septins. Nature 449, 311–315.

Sirajuddin M, Farkasovsky M, Zent E, Wittinghofer A (2009). GTP-induced conformational changes in septins and implications for function. Proc Natl Acad Sci USA 106, 16592–16597.

Steels JD, Estey MP, Froese CD, Reynaud D, Pace-Asciak C, Trimble WS (2007). Sept12 is a component of the mammalian sperm tail annulus. Cell Motil Cytoskeleton 64, 794–807.

Tada T, Simonetta A, Batterton M, Kinoshita M, Edbauer D, Sheng M (2007). Role of Septin cytoskeleton in spine morphogenesis and dendrite development in neurons. Curr Biol 17, 1752–1758.

Tsang CW, Estey MP, DiCiccio JE, Xie H, Patterson D, Trimble WS (2011). Characterization of presynaptic septin complexes in mammalian hippocampal neurons. Biol Chem 392, 739–749.

Tsang CW, Fedchyshyn M, Harrison J, Xie H, Xue J, Robinson PJ, Wang LY, Trimble WS (2008). Superfluous role of mammalian septins 3 and 5 in neuronal development and synaptic transmission. Mol Cell Biol 28, 7012–7029.

Weirich CS, Erzberger JP, Barral Y (2008). The septin family of GTPases: architecture and dynamics. Nat Rev Mol Cell Biol 9, 478–489.

Wittig I, Braun HP, Schagger H (2006). Blue native PAGE. Nat Protoc 1, 418–428.

Wu JQ, Ye Y, Wang N, Pollard TD, Pringle JR (2010). Cooperation between the septins and the actomyosin ring and role of a cell-integrity pathway during cell division in fission yeast. Genetics 186, 897–915.

Xie Y, Vessey JP, Konecna A, Dahm R, Macchi P, Kiebler MA (2007). The GTP-binding protein septin 7 is critical for dendrite branchin g and dendritic-spine morphology. Curr Biol 17, 1746–1751.

Xue J, Tsang CW, Gai WP, Malladi CS, Trimble WS, Rostas JA, Robinson PJ (2004). Septin 3 (G-septin) is a developmentally regulated phosphoprotein enriched in presynaptic nerve terminals. J Neurochem 91, 579–590.

Zent E, Vetter I, Wittinghofer A (2011). Structural and biochemical properties of Sept7, a unique septin required for filament formation. Biol Chem 392, 791–797.